

Electrochemistry of Room Temperature Protic Ionic Liquids: A Critical Assessment for Use as Electrolytes in Electrochemical Applications

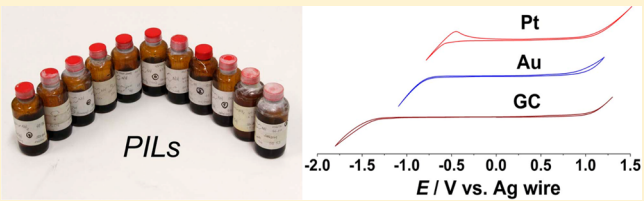
Xunyu Lu,[†] Geoff Burrell,[‡] Frances Separovic,[‡] and Chuan Zhao*,[†]

[†]School of Chemistry, The University of New South Wales, NSW 2052, Australia

[‡]School of Chemistry, Bio21 Institute, University of Melbourne, Victoria 3010, Australia

Supporting Information

ABSTRACT: Ten room temperature protic ionic liquids (RTPILs) have been prepared from low-molecular-weight Brønsted acids and amines with high purity and minimal water content, and their electrochemical characteristics determined using cyclic, microelectrode, and rotating disk electrode voltammetries. Potential windows of the 10 RTPILs were established at glassy carbon, gold, and platinum electrodes, where the largest potential window is generally observed with glassy carbon electrodes. The two IUPAC recommended internal potential reference systems, ferrocene/ferrocenium and cobaltocenium/cobaltocene, were determined for the 10 RTPILs, and their merits as well as limitations are discussed. Other electrochemical properties such as mass transport and double layer capacitances were also investigated. The potential applications of these RTPILs as electrolytes for electrochemical energy devices were discussed, and two novel applications using PILs for metal deposition and water electrolysis were demonstrated.



INTRODUCTION

Room temperature ionic liquids (RTILs) have been recognized as “green” solvents due to their negligible vapor pressure, nonflammability, as well as their outstanding solvation potential.¹ These unique properties make RTILs promising substitutes for conventional organic solvents. On the basis of their compositions, RTILs can be divided into three categories: aprotic ionic liquids, protic ionic liquids, and zwitterionic ionic liquids.² Protic ionic liquids (PILs) are formed by a variety of proton transfer and association equilibrium between neat Brønsted acids and bases. The very first PIL, as far as we are concerned, was ethanalammonium nitrate reported by Gabriel in 1888,³ which was also the first ionic liquid, having a melting point of 52–55 °C. The first room temperature PIL, ethylammonium nitrate (EAN), was reported by Walden in 1914 with a melting point of 12.5 °C.⁴ Since its discovery, EAN has become the focus of PIL investigation due to its water-like properties.

There is a growing interest in PILs in recent years. PILs often have lower melting points and glass transition temperatures and higher conductivities than their aprotic and zwitterionic counterparts.⁵ Importantly, PILs can be produced on a large scale at low cost due to the simplicity of their manufacture and the ubiquity of the starting materials, such as amines and acids. PILs also have the ability to form hydrogen bonds and hydrocarbon–solvent interactions and can act as proton acceptors as well as proton donors.⁶ Anouti et al. synthesized a series of PILs through neutralization reactions between pyrrolidine and Brønsted acids, and found these pyrrolidinium based PILs had relatively high conductivity, low toxicity, low cost, and large electrochemical windows and can be used as

media for thermal transfer and acid-catalyzed reactions.⁷ Wang et al. reported the preparation of a series of superbase-based PILs which were synthesized by proton transfer reaction between organic superbases and partially fluorinated alcohols; these PILs absorbed and released CO₂ rapidly.⁸ Martinelli et al. reported the preparation of 1-ethyl-3-methylimidazolium bis-(trifluoromethanesulfonyl)imide ([EMI][TFSI]) via neutralization between tertiary amines and *N,N*-bis-(trifluoromethanesulfonyl)imide. This type of PIL was introduced into a matrix based on a poly(vinylidene fluoride) (PVDF) copolymer to fabricate proton conducting membranes, where the relationship of conductivity and membrane stability at different PIL content ratios in the polymer matrix was studied.⁹ PILs also have been widely used in chromatography,¹⁰ self-assembly,^{6,11} and explosives.^{12,13}

Ionic liquids have been shown to exhibit advantages in electrochemical devices when applied as solvents and electrolytes. The potential windows of ILs can exceed 6 V, which is significant in comparison to conventional organic solvents containing supporting electrolytes (5.0 V for acetonitrile, 3.5 V for dichloromethane, and 4.4 V for dimethylsulfoxide).¹⁴ This property has made them very attractive for electrodeposition of metals that are not practicable in aqueous or organic electrolyte solutions. The intrinsic conductivity of ionic liquids means the addition of supporting electrolytes can be avoided, which makes reaction systems less complicated. The applications of PILs as electrolytes in electrochemical devices have mainly focused on

Received: May 15, 2012

Revised: June 26, 2012

Published: July 11, 2012

hydrogen–oxygen fuel cells where PILs have demonstrated advantages such as nonvolatility, wide electrochemical window, and high conductivity.¹⁵ Fuel cell systems with PILs thus can be fabricated without humidification, and are able to be operated above 100 °C. This would be most advantageous in small volume, high Pt electrode catalyst activity as well as reduced poisoning from carbon monoxide.¹⁶ These systems have better controllability in comparison to their humidified counterparts which only can be operated below 85 °C due to the volatile temperature of water.^{9,17,18} Recently, application of PILs as electrolytes for electrodeposition of conducting polymers, such as polyaniline,¹⁹ and electrolysis of water also have been reported.²⁰

Despite their well recognized fundamental and practical significance, systematic accounts of the electrochemical properties of PILs, akin to aprotic ILs, remain largely unavailable. Recently we synthesized 18 PILs and studied the electrochemical characteristics of the 8 that are RTPILs using a range of voltammetric techniques.²¹ The conventional preparative method involves dilution of reagents in sufficient solvent to facilitate removal of the exothermic energy from the neutralization reaction followed by removal of solvent *in vacuo*. However, negative effects of vacuum on component ratios of a PIL, particularly those containing volatile starting reagents, were previously observed.²¹ More recently, a solvent-free method has been developed to produce PILs of known and predictable stoichiometry where the Brønsted acid and base reagents were mixed as neat liquids with vigorous stirring.²² The method allows for reproducible preparation of very dry, high-purity RTPILs from low-molecular-weight volatile reagents.

In this paper, 10 RTPILs were prepared using the lately developed method and a systematic study of their electrochemical properties was carried out. The 10 RTPILs were selected due to their relatively low viscosity, which presumably leads to better electrochemical performances as electrolytes. Potential windows, availability of internal potential references based on oxidation of ferrocene and reduction of cobaltocenium hexaphosphate, and double-layer capacitance were surveyed. The influences of different methods on obtaining steady state voltammetry in these PILs have also been studied. We also demonstrate two novel applications of the PILs as electrolytes for electrodeposition of silver nanoparticles and water electrolysis.

EXPERIMENTAL SECTION

Materials. Formic [HCOOH] and glacial acetic [AcOH] acids were obtained from Ajax Chemicals (Auckland, New Zealand). Diethylamine [Et₂NH], triethylamine [Et₃N], diethanolamine [(HOEt)₂NH], pyrrolidine [Pyrr], ethylenediamine [EDA], bis(2-methoxyethyl)amine [(MeOEt)₂NH], di-n-butylphosphate [(BuO)₂POOH], and methylsulfonic acid [MsOH] were obtained from Sigma-Aldrich (St Louis, MO). The purification of these reagents was carried out according to previous literature,²² and the details are not described here. All reagents were stored away from light under an inert atmosphere and degassed by bubbling nitrogen immediately before reaction. Acetonitrile (CH₃CN, Sigma-Aldrich), cobaltocenium hexafluorophosphate (Co(C₅H₅)₂PF₆ or CcPF₆, Strem, MA), ferrocene (Fe(C₅H₅)₂ or Fc, BDH, Australia), tetrabutylammonium hexafluorophosphate (Bu₄NPF₆, Sigma-Aldrich), and silver tetrafluoroborate (AgBF₄, Sigma-Aldrich) were used as

received. All other reagents were obtained from Sigma-Aldrich and used without further purification.

PIL Preparation and Characterization. The 10 RTPILs were prepared according to a previous procedure.²² Briefly, the starting reagents were purified, dried, and handled under an inert atmosphere. The equivalent values of neat Brønsted acids as well as Brønsted bases were then added into the reactor simultaneously while stirring vigorously to dissipate the exothermic reaction heat. The addition rate was determined by the reaction volume and was set between 0.2 and 10 mL min⁻¹. The prepared PIL samples were highly pure, as confirmed by ¹H NMR and ¹³C NMR, with minimal water content in the range of ~100 ppm.

¹H NMR and ¹³C NMR measurements of these protic ionic liquids were acquired immediately after their preparation. Measurements of neat liquid samples were acquired with a Varian (Palo Alto, CA) INOVA 500 MHz NMR spectrometer. The neat liquids were transferred under an inert atmosphere to a standard 5 mm NMR tube and equipped with a Wilmad (Buena, NJ) NMR coaxial capillary insert of 60 μL volume containing 1% (w/w) sodium 3-(trimethylsilyl)propionic acid-*d*₄ acid (TSP) in D₂O solution as a reference/lock solution. ¹H and ¹³C spectra were externally referenced to TSP as 0 ppm.

Electrochemical Characterization Procedures. Voltammetric studies were undertaken on a CHI 760 Electrochemical Workstation (CH Instrument, Taxes). The glassy carbon (GC) disk electrode and the gold (Au) and platinum (Pt) disk working electrodes were purchased from CH instrument (CH Instrument, Taxes). Before each experiment, these working electrodes were polished with 0.3 μm alumina (Buehler, IL) mixed with water on a clean polishing cloth (Buehler). The polished electrodes were then rinsed with water and acetone and dried with lint free tissue paper. The areas of these working electrodes were calculated by analyzing cyclic voltammograms obtained by the peak current from oxidation of 1 mM ferrocene (Fc) in acetonitrile (0.1 M Bu₄NPF₆) using the Randles–Sevcik equation,²¹ eq 1,

$$i_p = 0.4463nF(nF/RT)^{1/2}AD^{1/2}\nu^{1/2}C \quad (1)$$

where *i*_p is the peak current (A), *n* = 1 is the number of electrons transferred in the oxidation of Fc, *A* is the area of the working electrodes (cm²), *D* = 2.3 × 10⁻⁵ cm² s⁻¹²³ is the diffusion coefficient in this system, *v* is the scan rate (V s⁻¹), and *C* is the concentration of Fc (mol cm⁻³). Other symbols have their own universal definitions. The calculated area of the working electrodes is 0.02 cm² for GC electrode, 0.035 cm² for Au electrode, and 0.037 cm² for Pt electrode.

Microelectrode measurements were undertaken with RAM electrodes (random assemblies of microdisks) which have surfaces that are inlaid with 7 μm diameter carbon fibers that are adequately spaced to avoid overlap of diffusion layers. A full description of the theory that underpins their operation, including the procedure for determining the number of active electrodes in each assembly, is available in the literature.^{24,25} Rotating disk voltammetric experiments were carried out with the CHI 760 Electrochemical Workstation in conjunction with a BAS MF-2066 glassy carbon rotating disk working electrode (working area = 0.162 cm²).

Voltammetric measurements of the PILs were carried out in a gastight electrochemical cell as described previously.²⁶ Before each test, 1 mL of dry PIL was transferred into the cell inside a nitrogen-filled glovebox. Cobaltocenium hexafluorophosphate and ferrocene are poorly soluble in some PILs, and an

ultrasonic bath (Unisonics Pty Ltd., Australia) was employed to assist with the dissolution for those compounds. All voltammetric experiments were carried out at room temperature (20 °C).

Other Characterization Procedures. Scanning electron microscopy (SEM) measurement of electrodeposition of silver was carried out with a FEI Nova NanoSEM 230 FESEM (field emission SEM, FEI, Oregon) at 15 kV. For water electrolysis experiment, platinum meshes were used as the working and counter electrodes and a Ag/AgCl (3 M NaCl) electrode was used as the reference electrode. Oxygen produced at the anode was detected by a fluorescent oxygen sensor (Oceanic Optics, Florida), and hydrogen generated at the cathode was confirmed by gas chromatography (GC, Thermo Focus DSQ, FL).

RESULTS AND DISCUSSION

Physical Properties of the As-Prepared PILs. In this investigation, a series of protic substituted ammonium salts were produced from secondary or tertiary amine bases with either organic or inorganic acids. Thermal properties, including glass transition temperature (T_g) and melting point (T_m), and physical properties such as density, viscosity, and ionic conductivity were reported in our previous study²² and are briefly summarized in Table 1.

Table 1. Physical and Thermal Properties of the 10 PILs

PILs	ρ (g/mL)	η (cP)	σ (mS cm ⁻¹)	T_g (°C)	T_m (°C)
[Pyrr][HCOOH] ^a	1.050	15.4	20.05		10.6
[Pyrr][AcOH] ^a	1.067	36.3	3.02		30.7
[EDA][HCOOH] ^a	1.107	112	9.83	-85.7	
[EDA][AcOH] ^a	1.103	958	0.59	-71.1	
[(MeOEt) ₂ NH] [HCOOH]	1.062	10.1	1.05	-85.31	4.6
[(MeOEt) ₂ NH] [AcOH]	1.045	15.2	1.03	-82.65	5.9
[(HOEt) ₂ NH] [(BuO) ₂ POOH] ^a	1.110	2409	0.06	-71.4	28.8
[Et ₂ NH] [(BuO) ₂ POOH] ^a	1.009	201	0.08	-89.9	-6.8
[Et ₃ N][MsOH] ^a	1.135	100	1.91	-78.9	24.3
[Et ₃ N] [(BuO) ₂ POOH] ^a	1.007	94.4	0.23	-91.0	

^aData from ref 22.

In one series, pyrrolidine ([Pyrr]) was combined with one equivalent of acetic ([AcOH]) or formic ([HCOOH]) acids. Initially, [Pyrr] was employed, as this cation is known to reduce both the melting point and viscosity of the ionic liquid.⁷ The formate and acetate compounds had comparatively low viscosity as well as low T_m values (Table 1). As these are desirable physical properties for reactive ionic liquids, the formic and acetic acids were then paired with other bases to determine which physical properties were due to the anion. In another series, [AcOH] and [HCOOH] acids were combined with two other different amine bases: ethylenediamine ([EDA]) and bis(2-methoxyethyl)amine ([MeOEt)₂NH]). The combination of [AcOH] and [HCOOH] acids with [EDA] leads to higher viscosity values, which were 958 and 112 cP, respectively, while their T_g values were still very low. However, the introduction of methoxy groups leads to a significant decrease in viscosity, as shown by [(MeOEt)₂NH][HCOOH] and [(MeOEt)₂NH][AcOH] that have a viscosity

of only 10.1 and 15.2 cP, which are the lowest among these PILs.

Then, diethylamine [Et₂NH], triethylamine [Et₃N], and diethanolamine [(HOEt)₂NH] were combined with di-n-butylphosphate [(BuO)₂PO₂H] and methylsulfonic acid [MsOH]. Compared to those PILs obtained with [AcOH] and [HCOOH] acids, PILs based on [(BuO)₂PO₂H] and [MsOH] acids have relatively lower conductivities, while their T_g and T_m are similar.

After the preparation of these PILs, a small portion was dissolved in D₂O and analyzed by ¹H and ¹³C NMR spectra immediately to ensure that no side reactions had occurred or unexpected molecular species formed. Chemical shifts of the ionized species in ionic liquids were dependent on concentration, and therefore, NMR was only used for rapid qualitative analysis. ¹H NMR and ¹³C NMR spectra of [Et₃N][MsOH] are shown in Figure S1 of the Supporting Information. As seen in Figure S1(a) (Supporting Information), δ_H at 1.45, 2.61, 3.30, and 9.45 ppm belong to protons in CH₃–, CH₃SO₃–, –CH₂N, and –SO₃H groups of Et₃N–CH₃SO₃H, respectively, and ¹³C NMR further confirms the structure. Peaks at 9.1, 40.0, and 47.2 ppm in Figure S1(b) (Supporting Information) are attributed to carbons in –CH₃, –CH₂N, and CH₃SO₃H groups. The clean baseline of the NMR spectra confirmed the high purity.

Conductivity is a very important parameter to assess the potential application of PILs in electrochemical devices. In many cases, the conductivity of ILs is associated with viscosity and lower viscosity typically endows ILs with higher conductivity. However, among the 10 PILs prepared here, the type of anions demonstrated more relevance to conductivity rather than the value of the viscosity. As seen in Table 1, PILs with [(BuO)₂PO₂H] anion had the lowest conductivity of these PILs. For example, [Et₃N][(BuO)₂PO₂H] has a viscosity of 94.4 cP and only has a conductivity of 0.23 mS cm⁻¹, much lower than PILs with similar viscosity. PILs with [HCOOH] anions have relative high conductivities compared to other anions in our study. [Pyrr][HCOOH] and [EDA][HCOOH] with a conductivity of 20.05 and 9.83 mS cm⁻¹, respectively, were the highest among the PILs prepared in this study.

Development of Reference Potential Scale in PILs. Lack of a standard reference electrode is a common issue in ionic liquid electrochemistry. In our voltammetric studies of PILs, a silver wire was often used as a quasi reference electrode. However, there is no defined thermodynamic significance in its potential notable to provide a usable reference point.^{27,28} As a result, it is difficult to compare potentials in different PILs using this reference electrode. Different types of conventional reference electrodes have been constructed and evaluated by several groups, including reference electrodes of the first kind (Ag/Ag⁺ couple dissolved in the ionic liquid) and of the second kind (Ag/AgCl in ionic liquids containing either dissolved Ag⁺ or Cl⁻).²⁸ However, no data are available based on use of conventional reference electrodes in PILs. Clearly, in principle, these types of reference electrodes may be fabricated in PILs where Ag salts are soluble or where the anions are, for example, halides or sulfate, which could be considered in future studies.

In order to compare voltammetric data obtained in different RTPILs, the IUPAC recommended ferrocene/ferrocenium (Fc⁰/Fc⁺) couple has been widely used as an internal potential reference in voltammetric studies in conventional nonaqueous media containing electrolytes.²⁹ This redox couple also has been widely used in RTILs.³⁰ In addition, the Cc^{+/-} redox

Table 2. Cyclic Voltammetric Data Obtained at a GC Electrode for Oxidation of Ferrocene and Reduction of Cobaltocinium Hexafluorophosphate in PILs

PILs	scan rate (mV s ⁻¹)	Cc ^{+/-}			Fc ^{0/+}		
		ΔE _p (mV)	i _{p,a} /i _{p,c}	D (cm ² s ⁻¹)	ΔE _p (mV)	i _{p,a} /i _{p,c}	D (cm ² s ⁻¹)
[Pyrr][HCOOH]	50	66	1.01	1.79 × 10 ⁻⁶	96	1.12	1.69 × 10 ⁻⁶
	500	75	0.97	1.75 × 10 ⁻⁶	95	1.06	1.75 × 10 ⁻⁶
[Pyrr][AcOH]	100	55	0.60	d	c	c	c
	300	58	0.64	d	c	c	c
[EDA][HCOOH]	50	56	0.99	9.72 × 10 ⁻⁷	b	b	b
	300	71	1.01	1.08 × 10 ⁻⁶	b	b	b
[EDA][AcOH]		b	b	b	b	b	b
		b	b	b	b	b	b
[(HOEt) ₂ NH][(BuO) ₂ POOH]		c	c	c	b	b	b
		c	c	c	b	b	b
[(MeOEt) ₂ NH][HCOOH]	50	132	0.43	d	179	1.23	1.96 × 10 ⁻⁶
	300	219	0.56	d	203	1.01	6.69 × 10 ⁻⁷
[(MeOEt) ₂ NH][AcOH]	200	65	0.47	d	96	1.20	7.14 × 10 ⁻⁷
	500	73	0.57	d	109	1.17	7.19 × 10 ⁻⁷
[Et ₃ N][(BuO) ₂ POOH]		c	c	c	a	a	a
		c	c	c	a	a	a
[Et ₃ N][MsOH]	30	62	0.99	4.87 × 10 ⁻⁸	68	1.10	6.70 × 10 ⁻⁸
	300	68	0.98	4.31 × 10 ⁻⁸	73	1.11	6.35 × 10 ⁻⁸
[Et ₂ NH][(BuO) ₂ POOH]	500	c	c	c	285	1.01	4.84 × 10 ⁻⁷
	1000	c	c	c	362	1.03	3.57 × 10 ⁻⁷

^aThe oxidation peak of Fc overlapped with the anodic potential limits of the ionic liquids. ^bCc⁺, Fc is insoluble for measurements of parameters.

^cThe redox process of Cc^{+/-} or Fc^{0/+} is irreversible. ^dElectrochemically irreversible process. The ratios cannot be calculated.

couple has been verified to be a useful internal potential reference standard in both organic solvents as well as RTILs by Bond and co-workers.^{31,32} In our study, the two redox processes, Fc^{0/+} and Cc^{+/-}, were tested for the 10 PILs using cyclic voltammetry at a GC working electrode. The results are summarized in Table 2.

Fc^{0/+} as an Internal Potential Reference. Figure 1a shows the cyclic voltammogram (CV) obtained at a GC electrode for oxidation of 3 mM Fc in [Et₃N][MsOH] at scan rates from 0.03 to 0.3 V s⁻¹. Reversible voltammetric behavior was observed. The ratio of the oxidation peak i_{p,a} to the reduction peak i_{p,c} was close to unity which confirms the reversibility of this process. At slow scan rates (<100 mV s⁻¹), the peak separations ΔE_p ($\Delta E_p = E_{p,a} - E_{p,c}$) were around 68 mV, which is very close to the theoretical value of 56 mV for a one-electron reversible process at 20 °C.³¹ ΔE_p became larger as expected when the scan rate increased (>200 mV) which is due to the enhanced impact of Ohmic drop. Moreover, $E^{\circ} = (E_{p,a} + E_{p,c})/2$ was independent of scan rate, also indicating a reversible process. A linear relationship of the peak current (i_p) and the square root of scan rate ($v^{1/2}$) was found, which confirms the process is diffusion controlled. The diffusion coefficient of Fc in [Et₃N][MsOH] calculated from the Randles–Sevcik relationship was 6.70×10^{-8} cm² s⁻¹, which is much smaller than Fc in conventional solvents such as CH₃CN (1.9×10^{-5} cm² s⁻¹) but much higher than that in viscous aprotic IL, e.g., [BMIM][PF₆] (1×10^{-8} cm² s⁻¹).¹⁴

Figure 1b shows the CVs of oxidation of 3 mM Fc in [(MeOEt)₂NH][AcOH] with a GC electrode. At slow scan rates (<0.2 V s⁻¹), the voltammetric responses were chemically irreversible. At the scan rate of 0.03 V s⁻¹, a well-shaped oxidation peak can be observed at 0.672 V vs Ag wire, while in the reverse scan, no reduction peak was detected in the reverse scan. However, when the scan rate was increased to above 0.2 V s⁻¹, the voltammetric responses became reversible, suggesting

an EC mechanism for the oxidation of Fc⁰ to Fc⁺ in [(MeOEt)₂NH][AcOH].²¹

A common issue for using Fc as the internal potential reference is the poor solubility of Fc in many PILs such as [EDA][HCOOH]. Moreover, the oxidation potential of Fc⁰ is very close to the anodic potential limit of some PILs, thus deteriorating the reversibility of the Fc^{0/+} process and making the evaluation of the reversible potential difficult. Figure 1c shows an example of the Fc^{0/+} process in [Pyrr][AcOH]. Irreversible voltammetric behavior was observed, presumably because Fc⁺ reacts with the IL itself or the oxidation products of the IL. Similar irreversible behavior of Fc also has been observed in other PILs.²¹ In these circumstances, the Fc^{0/+} couple becomes unsuitable to be used as an internal potential reference.

Cc^{+/-} as an Internal Potential Reference. Cc^{+/-} appears to be a useful alternative to Fc^{0/+} as the internal potential reference for PILs and shows better solubility and reversibility than Fc in many ILs.³³ Figure 2a shows a typical cyclic voltammogram obtained at a GC electrode for reduction of 3 mM Cc⁺ in [Et₃N][MsOH] at different scan rates. Reversible voltammetric behavior for the reduction of Cc⁺ was observed. At slow scan rates (<0.2 V s⁻¹), the peak separations ΔE_p were around 60 mV, which is very close to the theoretical value of 56 mV.³¹ Moreover, $E^{\circ} = (E_{p,a} + E_{p,c})/2$ was independent of scan rate, also indicating a reversible process. A linear relationship of the peak current (i_p) and the square root of scan rate ($v^{1/2}$) was found, which again confirms this process is diffusion controlled.

A problem was encountered when Cc^{+/-} was applied as an internal potential reference in all PILs containing di-n-butylphosphate [(BuO)₂POOH] anions. As seen in Figure 2b, only the reduction peaks of Cc⁺ in [Et₃N][(BuO)₂POOH] and no oxidation peak was observed at a scan rate up to 0.5 V s⁻¹. An analogous phenomenon was observed in the other three [(BuO)₂POOH] anion-based PILs, namely, [(HOEt)₂NH]-

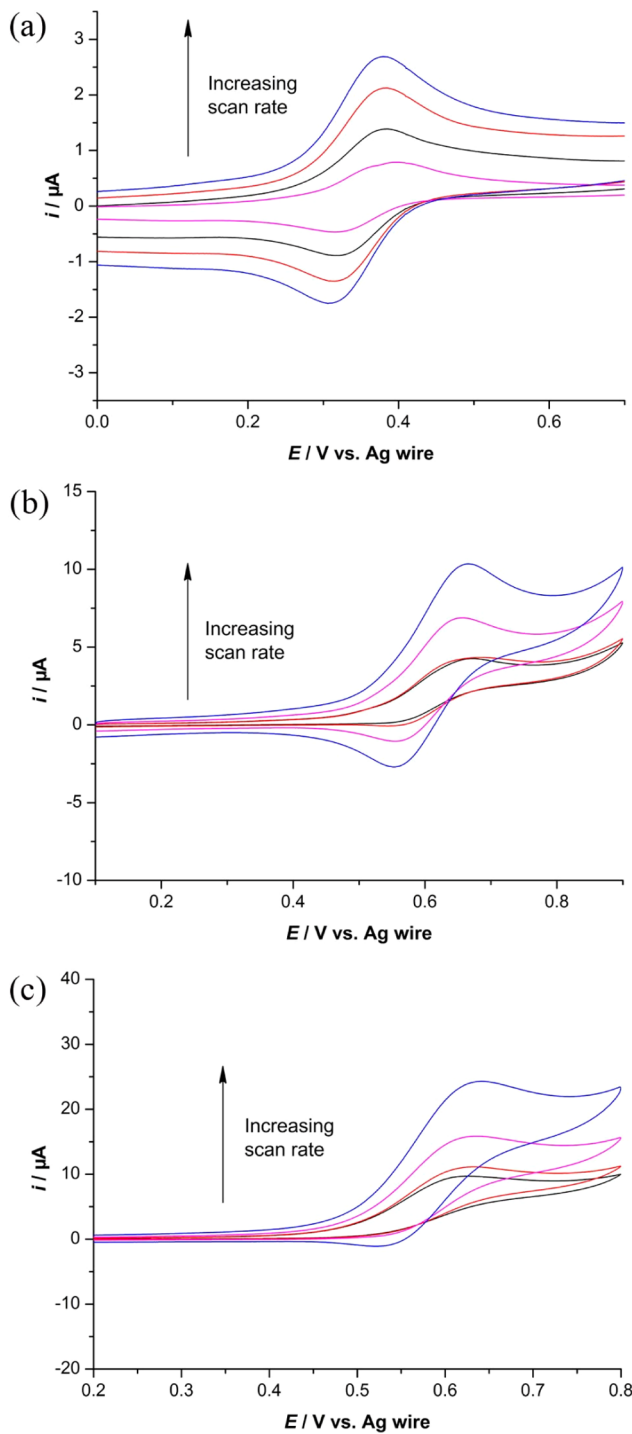


Figure 1. Cyclic voltammograms obtained for the oxidation of 3 mM Fc with a glassy carbon electrode in (a) $[\text{Et}_3\text{N}][\text{MsOH}]$ at a scan rate of 0.03, 0.1, 0.2, and 0.3 V s^{-1} , respectively, (b) $[(\text{MeOEt})_2\text{NH}][\text{AcOH}]$ at a scan rate of 0.03, 0.05, 0.2, and 0.5 V s^{-1} , respectively, and (c) $[\text{Pyrr}][\text{AcOH}]$ at a scan rate of 0.03, 0.2, 0.3, and 1 V s^{-1} , respectively.

$[(\text{BuO})_2\text{POOH}]$, $[\text{Et}_3\text{N}][(\text{BuO})_2\text{POOH}]$, and $[\text{Et}_2\text{NH}][(\text{BuO})_2\text{POOH}]$. As the $\text{Cc}^{+/0}$ process was irreversible, it cannot be used as an internal potential reference for $[(\text{BuO})_2\text{POOH}]$ anion-based PILs.

Conversion between Two Internal Potential References. Table 2 shows that for many PILs only one of the two IUPAC recommended internal potential references, $\text{Fc}^{0/+}$ and $\text{Cc}^{+/0}$,

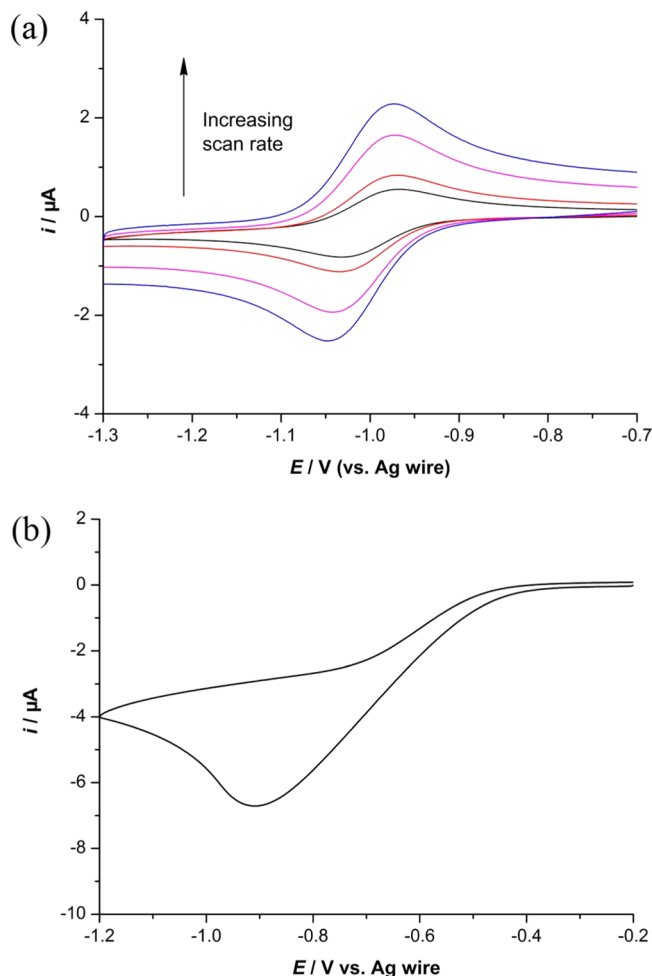


Figure 2. Cyclic voltammograms obtained with a glassy carbon electrode: (a) for the reduction of 3 mM Cc^+ in $[\text{Et}_3\text{N}][\text{MsOH}]$ at a scan rate of 0.05, 0.1, 0.3, and 0.5 V s^{-1} , respectively, and (b) for the reduction of 2 mM Cc^+ in $[(\text{MeOEt})_2\text{NH}][\text{AcOH}]$ at a scan rate of 0.1 V s^{-1} .

could be applied. The lack of a common standard has made comparison of potentials obtained in different PILs difficult. Previous studies have found that in aprotic ionic liquids (AILS) the potential separation between $\text{Fc}^{0/+}$ and $\text{Cc}^{+/0}$ is a constant and also independent of the solvent used.^{34,35} Figure 3 shows the cyclic voltammogram obtained at a GC electrode for the PIL $[\text{Et}_3\text{N}][\text{MsOH}]$ containing an equal molarity of Fc^0 and Cc^+ (2 mM). Both the oxidation of Fc^0 and reduction of Cc^+ were found to be reversible with their reversible formal potentials at 0.214 and -1.126 V, respectively. This results in a potential separation of 1.34 V between the two processes. The same value was also obtained with other PILs, where both Fc and Cc^+ can be applied as an internal reference standard.

On the basis of the above observations, the relationship between the two internal potential references, $\text{Fc}^{0/+}$ and $\text{Cc}^{+/0}$, can be described by using eq 2

$$E (\text{vs } \text{Cc}^{+/0}) = E (\text{vs } \text{Fc}^{0/+}) + 1.34 \text{ V} \quad (2)$$

where $E (\text{vs } \text{Cc}^{+/0})$ is the potential referenced against $\text{Cc}^{+/0}$, while $E (\text{vs } \text{Fc}^{0/+})$ is the potential referenced against $\text{Fc}^{0/+}$. For example, in $[(\text{BuO})_2\text{POOH}]$ anion-based PILs where $\text{Cc}^{+/0}$ cannot be used as an internal reference owing to the irreversibility, the potential values obtained against $\text{Fc}^{0/+}$ can

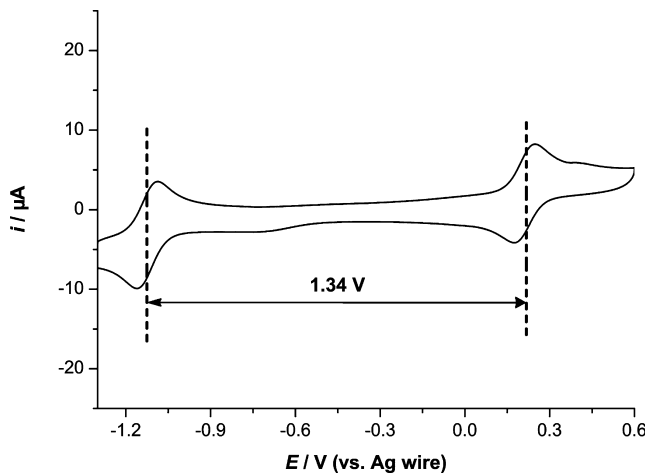


Figure 3. Cyclic voltammograms obtained in $[\text{Et}_3\text{N}][\text{MsOH}]$ at a scan rate of 0.1 V s^{-1} with a glassy carbon electrode containing $2 \text{ mM } \text{Cc}^{+}$ and $2 \text{ mM } \text{Fc}$.

still be converted by using eq 2 and compared with other PILs where $\text{Cc}^{+/-}$ can be used as an internal reference.

Potential Window. Potential window is an important indicator of electrochemical stability of RTILs. Parameters that affect the potential windows of ionic liquids are complicated. Besides their electrochemical stability, the interaction between anions and cations also plays an important role in determining the potential windows of ionic liquids. Strong intermolecular effects, such as hydrogen bonding and ion–ion interactions, are also said to modify the physicochemical properties of PILs.²¹ The electrochemical potential windows of the 10 PILs were examined by using cyclic voltammetry at a scan rate of 0.1 V s^{-1} at GC, Au, and Pt working electrodes. Table 3 summarizes the cathodic and anodic potential limits of the 10 PILs. $\text{Cc}^{+/-}$ and/or $\text{Fc}^{0/+}$, wherever applicable, were applied as internal potential references, and all the data were either referred to the $\text{Fc}^{0/+}$ process directly or using eq 2.

Figure 4 shows typical potential windows obtained at Pt, Au, and GC working electrodes in a PIL $[(\text{MeOEt})_2\text{NH}][\text{AcOH}]$. The largest potential window was obtained with the GC working electrode. The anodic limit was at 1 V vs Ag wire presumably owing to the oxidation of $[\text{Ac}]$ anions, while the cathodic limit reached -1.37 V vs Ag wire, which could be ascribed to the reduction of $[(\text{MeOEt})_2\text{NH}]$ cations but also possibly to the reduction of protons. At a Au working electrode, $[(\text{MeOEt})_2\text{NH}][\text{AcOH}]$ showed a cathodic limit of 0.87 V vs Ag wire which is close to that obtained at GC working electrodes. However, the anodic limit from the Au working electrode was much smaller than that of the GC working electrode. The potential windows obtained at a Pt working electrode were similar to those obtained with a Au electrode.

Table 3 and Figure 4 show that the electrode material has a strong effect on the potential windows. The largest potential window was always obtained with GC electrodes. In some occasions, Au and Pt electrodes exhibited anodic limits close to that of GC electrodes and sometimes even larger anodic limits. However, Au and Pt electrodes usually had smaller cathodic potential limits than GC electrodes. The reason could be that noble metal electrodes such as Pt and Au are more sensitive (smaller overpotentials) to the reduction of protons as well as impurities (e.g., water), similar to effects often observed in

conventional organic solvents, aprotic ionic liquids, and other PILs.^{21,36,37}

Angell et al.^{38–40} have suggested that the relative difference in aqueous pK_a between the acid and base components of PILs can provide a useful measure for predicting the proton transfer and physicochemical properties of PILs. However, a graph of ΔpK_a versus electrochemical windows showed essentially no correlation. Furthermore, a direct correlation between ionic (amine/acid) structure and electrochemical windows was not observed. The cathodic and anodic limiting potential varies even for the same cation or anion. These results reflect complex interactions such as ion mobility, hydrogen bonding, and ion–ion interactions that can dramatically affect the electrochemical properties of PILs.^{11,21}

Among the 10 PILs prepared here, $[\text{Et}_3\text{N}][\text{MsOH}]$ had potential windows of 4.73 , 2.83 , and 2.47 V with GC, Au, and Pt electrodes, respectively. These values of potential windows were the widest of the 10 PILs, which makes it favorable to be used as an electrolyte for applications such as water electrolysis systems or fuel cells.

Double Layer Capacitance. Electric double layer capacitors (EDLCs) are important energy storage devices and have attracted great research interests owing to their desirable properties such as long cycle life, high power density, and their “green” nature (e.g., absence of heavy metal materials).⁴¹ To improve the performance of EDLCs requires electrolytes with high power density as well as high temperature stability. Due to properties described earlier in this work, ILs are attractive electrolytes for EDLCs and a high capacity can be expected because of the high concentrations ($3\text{--}5 \text{ M}$) of ion species that contribute to the double layer formation. Furthermore, the nonflammability of ILs presents an attractive feature for the enhanced safety of EDLCs. Previously, imidazolium- and phosphonium-based AILs were used as novel electrolytes for EDLCs due to these merits.^{42,43}

In this study, the double layer capacitances of the 10 PILs were tested and the possibility of applying them as EDLCs was evaluated. The capacitance of the 10 PILs was measured with a GC working electrode according to eq 3

$$i_c = C_{dl}v \quad (3)$$

where i_c is the double layer charging current when there is no Faradic current, C_{dl} is the double layer capacitance per unit area, and v is the scan rate. Under ideal conditions, C_{dl} can be calculated by the slope from a plot of i_c versus v . The largest value of C_{dl} was found to be $70.6 \mu\text{F cm}^{-2}$ from $[\text{Pyrr}][\text{HCOOH}]$, which also has the lowest viscosity among the 10 PILs. C_{dl} obtained using more viscous PILs were generally smaller than those obtained in less viscous PILs. For instance, the viscous PILs $[\text{Et}_2\text{NH}][(\text{BuO})_2\text{POOH}]$ and $[(\text{HOEt})_2\text{NH}][(\text{BuO})_2\text{POOH}]$ had comparatively much lower C_{dl} values of 15.3 and $19.4 \mu\text{F cm}^{-2}$, respectively.

Among the 10 PILs, $[\text{Pyrr}][\text{AcOH}]$, $[\text{Pyrr}][\text{HCOOH}]$, $[(\text{MeOEt})_2\text{NH}][\text{AcOH}]$, $[(\text{MeOEt})_2\text{NH}][\text{HCOOH}]$, and $[\text{Et}_3\text{N}][\text{MsOH}]$ showed high C_{dl} values, good conductivity (Table 1), and relatively large electrochemical potential windows (Table 3), which suggests they are potentially usable electrolytes for high energy density EDLCs. However, the C_{dl} values obtained above were based on the Stern-diffuse double layer model, which has been widely applied in the interface of aqueous–electrode–electrolyte.³⁶ This model is not necessarily applicable to the ionic liquids, and studies have suggested that a multilayer model could be preferable for ionic liquids.⁴⁴

Table 3. Potential Windows Obtained with 10 PILs at Different Electrodes

PILs	electrode material	anodic limit (V)	cathodic limit (V)	potential windows (V)	potential reference
[Pyrr][HCOOH]	GC	0.66	-1.89	2.55	$\text{Fc}^{0/+}$
	GC	1.04	-1.51	2.55	Ag wire
	Au	0.95	-0.87	1.82	Ag wire
	Pt	1.08	-0.37	1.45	Ag wire
[Pyrr][AcOH]	GC	0.32	-2.33	2.65	$\text{Fc}^{0/+}$
	GC	0.87	-1.78	2.65	Ag wire
	Au	0.90	-0.97	1.87	Ag wire
	Pt	0.92	-0.68	1.60	Ag wire
[EDA][HCOOH]	GC	0.19	-2.56	2.75	$\text{Fc}^{0/+}$
	GC	1.02	-1.73	2.75	Ag wire
	Au	0.18	-0.88	1.06	Ag wire
	Pt	1.23	-0.50	1.73	Ag wire
[EDA][AcOH]	GC	b	b	b	$\text{Fc}^{0/+}$
	GC	0.89	-1.87	2.76	Ag wire
	Au	0.58	-0.90	1.48	Ag wire
	Pt	1.42	-1.03	2.45	Ag wire
[(HOEt) ₂ NH][(BuO) ₂ POOH]	GC	b	b	b	$\text{Fc}^{0/+}$
	GC	0.79	-2.05	2.84	Ag wire
	Au	0.64	-0.93	1.57	Ag wire
	Pt	1.01	-0.62	1.63	Ag wire
[(MeOEt) ₂ NH][HCOOH]	GC	0.18	-2.06	2.24	$\text{Fc}^{0/+}$
	GC	0.84	-1.40	2.24	Ag wire
	Au	0.10	-0.62	0.72	Ag wire
	Pt	-0.06	-0.72	0.66	Ag wire
[(MeOEt) ₂ NH][AcOH]	GC	0.37	-2.00	2.37	$\text{Fc}^{0/+}$
	GC	1.00	-1.37	2.37	Ag wire
	Au	0.87	-0.79	1.66	Ag wire
	Pt	1.03	-0.59	1.62	Ag wire
[Et ₂ NH][(BuO) ₂ POOH]	GC	0.15 ^a	-2.79 ^a	2.94 ^a	$\text{Fc}^{0/+}$
	GC	0.85	-2.09	2.94	Ag wire
	Au	0.79	-0.89	1.68	Ag wire
	Pt	0.93	-0.68	1.61	Ag wire
[Et ₃ N][MsOH]	GC	1.69	-3.04	4.73	$\text{Fc}^{0/+}$
	GC	2.03	-2.70	4.73	Ag wire
	Au	1.93	-0.90	2.83	Ag wire
	Pt	2.05	-0.42	2.47	Ag wire
[Et ₃ N][(BuO) ₂ POOH]	GC	b	b	b	$\text{Fc}^{0/+}$
	GC	0.90	-1.76	2.66	Ag wire
	Au	0.83	-0.93	1.76	Ag wire
	Pt	0.93	-0.69	1.62	Ag wire

^aCalculated from $\text{Fc}^{0/+}$ using eq 2. ^b Cc^+ or Fc cannot be established due to the poor solubility or irreversible redox processes.

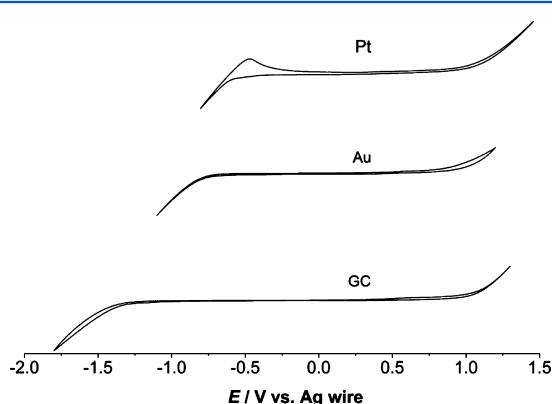


Figure 4. Electrochemical potential windows of $[(\text{MeOEt})_2\text{NH}][\text{AcOH}]$ obtained at platinum, gold, and glassy carbon electrodes at a scan rate of 0.1 V s^{-1} .

Nevertheless, PILs are still seen as suitable solvent electrolytes in electrochemical studies, since they have adequate capacitance values, good stability, and wide potential windows.

Steady-State Voltammetry. In all the above-mentioned electrochemical experiments using macrodisk electrodes, only transient responses were obtained. In principle, steady-state measurements based on rotating disk or microelectrode methods would minimize iR drop and background capacitance terms and thus would be valuable in PIL-based electrolytes. However, under conditions where steady-state responses can be obtained in aqueous and conventional organic solvent-electrolyte solutions, only transient responses are usually obtained in IL media, largely due to their high viscosity.

Figure 5a shows a series of rotating disk electrode (RDE) voltammograms of oxidation of 3 mM Fc in [Pyrr][HCOOH] obtained at different rotation rates. Without rotation, a typical transient response was obtained at a scan rate of 30 mV s^{-1} . When the rotation increased to 500 rpm, a peak-shaped

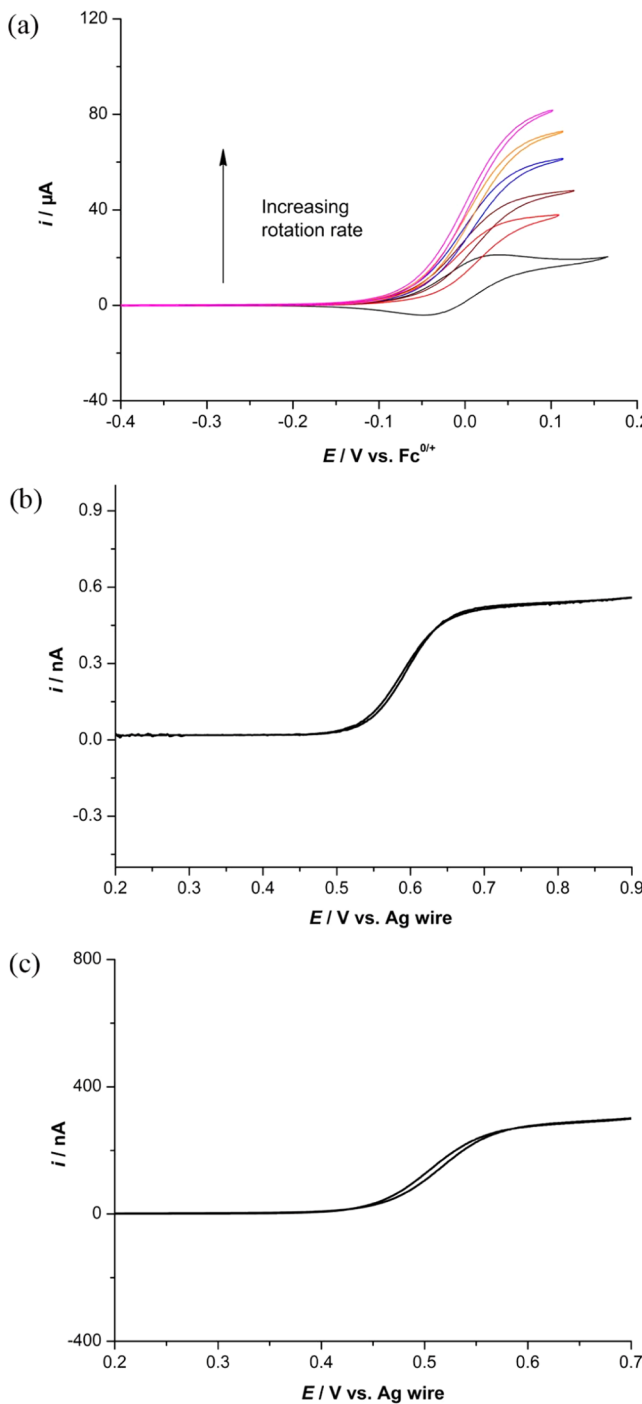


Figure 5. Cyclic voltammograms for oxidation of 3 mM Fc in [Pyrr][HCOOH] obtained at (a) a glassy carbon RDE at a scan rate of 0.03 V s^{-1} with rotating rates at 0, 500, 1000, 2000, 3000, and 4000 rpm, respectively, (b) a $1 \mu\text{m}$ radius Pt ultramicroelectrode at a scan rate of 0.01 V s^{-1} , and (c) a RAM electrode at a scan rate of 0.01 V s^{-1} .

transient rather than a sigmoidal curve was observed. This is due to the high viscosity and low diffusion coefficients of Fc in the PIL, which is only about $1.7 \times 10^{-6} \text{ cm}^2 \text{ s}^{-1}$ in [Pyrr][HCOOH] in comparison with $2.3 \times 10^{-5} \text{ cm}^2 \text{ s}^{-1}$ in acetonitrile.³⁰ Further increase of the rotation rate to above 1000 rpm eventually resulted in a steady-state response obtained in the PIL. Notably, [Pyrr][HCOOH] had the lowest viscosity (15.4 cP) among all 10 PILs studied, which enabled the steady state to be achieved at a relatively low rotation rate.

While in more viscous PILs, such as [EDA][HCOOH] (112 cP) and [Et₃N][MsOH] (100 cP), a rotation rate larger than 3000 rpm was required to achieve near steady-state response. However, as also observed in our previous studies, it is impractical to apply a high rotation rate in very viscous ionic liquids, as air bubbles can become incorporated at the surface of electrode, leading to very noisy signals.²¹

A common alternative solution to achieve steady-state measurement in viscous liquids is to use ultramicroelectrodes (UMEs).⁴⁵ When UMEs are used at slow scan rates, steady-state response could be obtained in PILs. Also, UMEs are used in a stationary state, which can eliminate the problems associated with mechanical rotation of the electrode. Figure Sb displays the voltammogram obtained at a $2 \mu\text{m}$ diameter platinum UME for oxidation of 3 mM Fc⁰ in [Pyrr][HCOOH] at a scan rate of 10 mV s^{-1} . In this less viscous PIL, steady state response could be relatively easily obtained. However, practical problems when using UMEs in viscous ILs are accurately measuring the very small current as a result of the small electrode size, the much smaller diffusion coefficients, and sometimes the very poor solubility of redox compounds in viscous ILs. We demonstrated recently the use of a random assembly microelectrode (RAM) array electrode in an AIL to achieve steady state measurement with high current.⁴⁶ Figure Sc shows a voltammogram obtained with a RAM electrode at a scan rate of 10 mV s^{-1} [Pyrr][HCOOH] containing 3 mM Cc⁺ and 3 mM Fc. The steady-state response was achieved, and the current obtained was $\sim 1\text{--}2$ orders of magnitude higher than that obtained with a single UME. Thus, large current steady-state measurement can be obtained in viscous PILs without the sacrifice of accuracy.

Electrochemical Applications of the PILs. PILs have drawn much recent attention as electrolytes in electrochemical applications. The combination of high ionicity, proton exchange kinetics, and relatively low vapor pressure make PILs excellent candidates for usage as fuel cell electrolytes, albeit concerns regarding evaporative loss of the ionic liquid remain. Specific capacitance, high conductivity, and wide electrochemical windows also suggest PILs are promising electrolytes for electrochemical capacitors. In this study, we demonstrated two novel electrochemical applications using the as prepared PILs as electrolytes for electrodeposition of metals and water electrolysis.

Electrodeposition of Silver. Protic ILs, as far as we know, have not been reported for metal electrodeposition. In comparison to AILs, PILs may seem less attractive for electrodeposition due to their protic nature and high hydrophilicity, which could, in principle, reduce the cathodic potential limit. Nevertheless, our studies have shown that many PILs can offer quite large cathodic potential windows up to $-3.04 \text{ V vs. } \text{Fc}^{0/+}$ (see Table 3 and also Table 4 in ref 21), which are comparable to aprotic ionic liquids. Furthermore, PILs usually can be prepared by simple synthetic routes from reagents easily available in industry and have a relatively lower cost compared to AILs. This advantage makes PILs more suitable for large scale applications.

In this paper, we carried out the electrodeposition of Ag from a PIL media [EDA][HCOOH] containing 20 mM silver tetrafluoroborate (AgBF₄). Figure 6a shows the cyclic voltammogram obtained at a GC electrode in [EDA][HCOOH] containing 20 mM AgBF₄. The reductive deposition of bulk Ag was observed as the cathodic peak which appeared at $0.6 \text{ V vs. Ag wire}$, while the anodic peak at

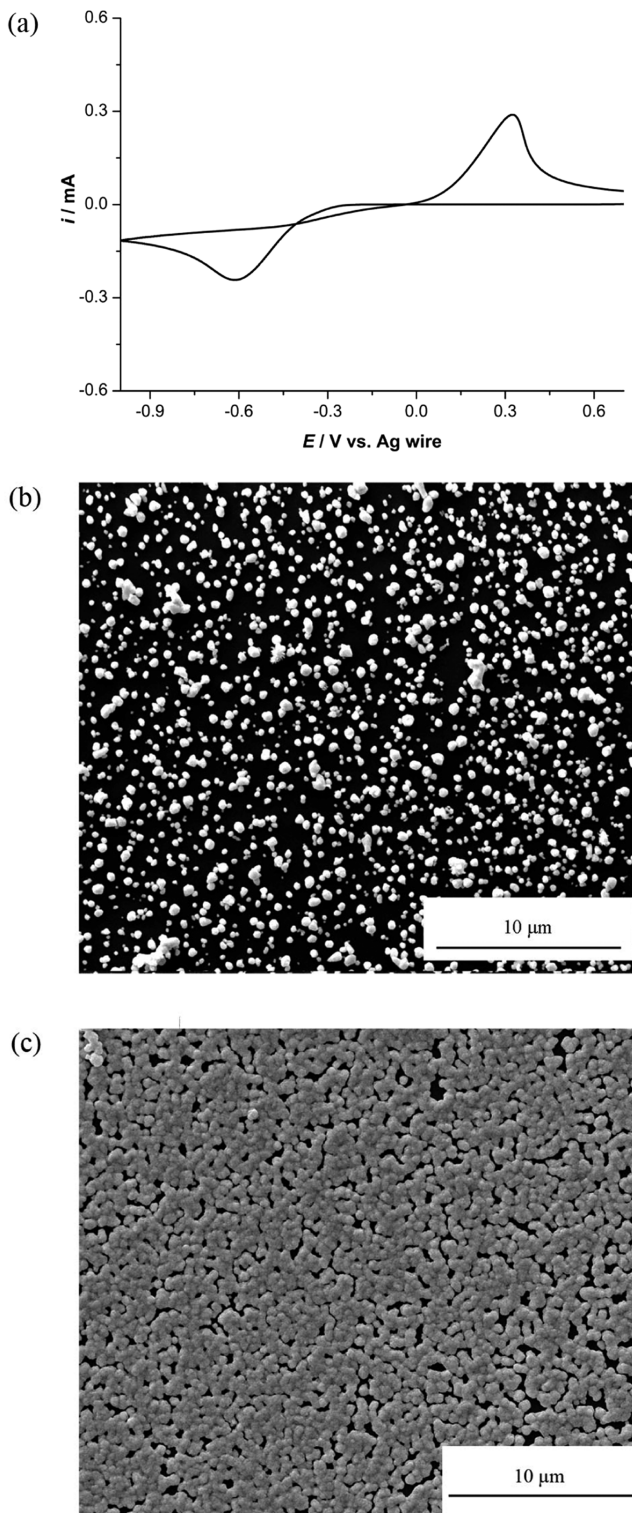


Figure 6. (a) Cyclic voltammogram obtained with a GC electrode in $[\text{EDA}][\text{HCOOH}]$ containing $20 \text{ mM} \text{AgBF}_4$ at a scan rate of 0.01 V s^{-1} . SEM analysis of silver nanoparticles deposited onto the ITO surface after (b) 20 cycles and (c) 100 cycles of CVs in the potential range of -1.1 to 0.9 V vs Ag wire.

about 0.3 V vs Ag wire represents the oxidative stripping of the deposited Ag back to Ag^+ . Figure 6b and c shows the SEM images of Ag nanoparticles deposited onto an ITO glass from $[\text{EDA}][\text{HCOOH}]$ by scanning potentials in the range of -1.1 to 0.9 V vs Ag wire at a scan rate of 0.1 V s^{-1} for 20 and 100

cycles, respectively. The images show that silver nanoparticles of diameters between 200 and 500 nm were obtained after 20 cycles. A uniform thin film composed of nanoparticles was formed on the surface of ITO when the deposition scan was increased to 100 cycles. EDX studies confirm that all the electrodeposited films are high purity silver.

Electrolysis of Water. Electrolysis of water to generate hydrogen and oxygen has been well-known for more than two centuries. Recently the technique has gained much renewed interests for production of hydrogen fuels, particularly by using electricity generated from renewable energy resources such as solar energy.⁴⁷ In this paper, we also explored the as-prepared PILs as novel electrolytes for water electrolysis to generate hydrogen and oxygen. An electrochemical cell (Figure S2, Supporting Information) was devised for water electrolysis reaction, of which the anode and cathode was separated by a piece of glass frit. The PIL $[\text{Et}_3\text{N}][\text{MsOH}]$ was selected owing to its excellent electrochemical stability, with a potential window close to 5 V , and high conductivity, particularly when mixed with water (37 mS cm^{-1} at 1 M concentration). Figure 7a shows the cyclic voltammogram obtained at a Pt

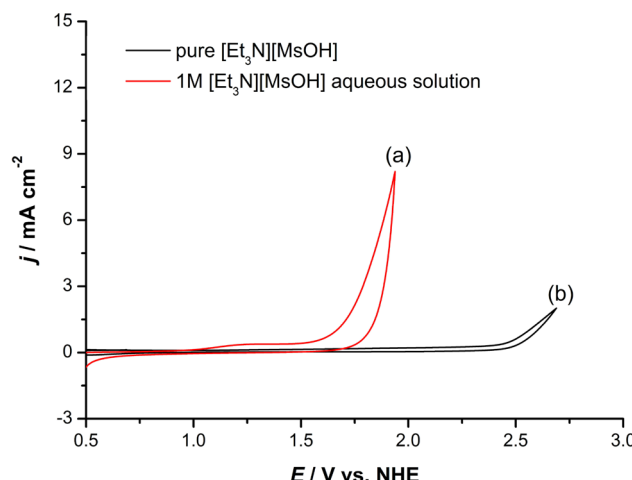


Figure 7. Cyclic voltammograms obtained with a Pt electrode at scan rate of 0.1 V s^{-1} in (a) $1 \text{ M} [\text{Et}_3\text{N}][\text{MsOH}]$ aqueous solution and (b) “neat” $[\text{Et}_3\text{N}][\text{MsOH}]$.

electrode at a scan rate of 0.1 V s^{-1} in $1 \text{ M} [\text{Et}_3\text{N}][\text{MsOH}]$ aqueous solution. The CV obtained in neat $[\text{Et}_3\text{N}][\text{MsOH}]$ using $\text{Fc}^{0/+}$ as an internal reference standard, and then converted against NHE (see the Supporting Information), was also included for comparison (Figure 7b). The anodic limit observed at $\sim 1.7 \text{ V}$ vs NHE (Figure 7a) in $1 \text{ M} [\text{Et}_3\text{N}][\text{MsOH}]$ aqueous solution is attributed to the oxidation of water to generate oxygen, which was confirmed by visual detection of gas bubble evolution and increase of oxygen concentration using an fluorescence oxygen sensor. The hydrogen evolution at the cathode was also visually detected and confirmed by gas chromatography. The small oxidation wave at 1.2 V on the anodic scan and the reductive peak at 0.4 V on the cathodic scan were attributed to the formation of platinum oxide and reductive stripping of platinum oxide back to Pt, respectively. In comparison, the PIL $[\text{Et}_3\text{N}][\text{MsOH}]$ itself has a much higher breakdown potential at around 2.5 V vs NHE (Figure 7b). Further studies of using PILs as electrolytes for water electrolysis are currently under way.

CONCLUSION

Ten room temperature PILs were synthesized and their electrochemical properties investigated. The two IUPAC recommended internal potential reference $\text{Fc}^{0/+}$ and/or $\text{Cc}^{+/0}$ redox processes were established for the PILs. The potential separation between the $\text{Fc}^{0/+}$ and $\text{Cc}^{+/0}$ redox processes was found to be always 1.34 V, which enables the conversion between the two internal potential references and thus makes useful comparisons. The diffusion coefficient of $\text{Cc}^{+/0}$ in these PILs was in the range of 10^{-6} – 10^{-8} $\text{cm}^2 \text{ s}^{-1}$, which is much smaller than that obtained in organic solvents due to the high viscosity of PILs. The potential windows of the 10 PILs were affected greatly by the material of electrodes, and the largest values were always observed at glassy carbon electrodes. Rotating disk, UME, and RAM electrodes were applied to achieve steady-state measurements in the viscous PILs. Two novel applications of these PILs as electrolytes for electrodeposition of metal and electrolysis of water were demonstrated in two PILs, $[\text{EDA}][\text{HCOOH}]$ and $[\text{Et}_3\text{N}][\text{MsOH}]$, respectively. This study provides a platform for further electrochemical applications of these ionic liquids, which have been shown to be technically important but not yet extensively used in electrochemical devices and industrial applications.

ASSOCIATED CONTENT

Supporting Information

Details of experimental setup, conversion of reference potential, and NMR spectra. This material is available free of charge via the Internet at <http://pubs.acs.org>.

AUTHOR INFORMATION

Corresponding Author

*E-mail: chuan.zhao@unsw.edu.au.

Notes

The authors declare no competing financial interest.

ACKNOWLEDGMENTS

The authors thank UNSW electron micro unit (EMU) analytical centre for access to SEM facilities. The study was financed by an ARC Discovery Grant (DP110102569).

REFERENCES

- (1) Welton, T. *Chem. Rev.* **1999**, *99*, 2071–2083.
- (2) Armand, M.; Endres, F.; MacFarlane, D. R.; Ohno, H.; Scrosati, B. *Nat. Mater.* **2009**, *8*, 621–629.
- (3) Gabriel, S. *Berichte* **1888**, *21*, 2664–2669.
- (4) Walden, P. *Bull. Acad. Imp. Sci. Petrograd.* **1914**, 1800–1808.
- (5) Duan, Z. Y.; Gu, Y. L.; Zhang, J.; Zhu, L. Y.; Deng, Y. Q. *J. Mol. Catal. A: Chem.* **2006**, *250*, 163–168.
- (6) Wang, J. Y.; Greaves, T. L.; Kennedy, D. F.; Weerawardena, A.; Song, G. H.; Drummond, C. J. *Aust. J. Chem.* **2011**, *64*, 180–189.
- (7) Anouti, M.; Cailllon-Caravanier, M.; Dridi, Y.; Galiano, H.; Lemordant, D. *J. Phys. Chem. B* **2008**, *112*, 13335–13343.
- (8) Wang, C. M.; Luo, H. M.; Jiang, D. E.; Li, H. R.; Dai, S. *Angew. Chem., Int. Ed.* **2010**, *49*, 5978–5981.
- (9) Martinelli, A.; Matic, A.; Jacobsson, P.; Borjesson, L.; Fernicola, A.; Panero, S.; Scrosati, B.; Ohno, H. *J. Phys. Chem. B* **2007**, *111*, 12462–12467.
- (10) Poole, C. F. *J. Chromatogr., A* **2004**, *1037*, 49–82.
- (11) Greaves, T. L.; Weerawardena, A.; Fong, C.; Drummond, C. J. *J. Phys. Chem. B* **2007**, *111*, 4082–4088.
- (12) Galvez-Ruiz, J. C.; Holl, G.; Karaghiosoff, K.; Klapotke, T. M.; Lohnwitz, K.; Mayer, P.; Noth, H.; Polborn, K.; Rohrbogner, C. J.; Suter, M.; Weigand, J. *J. Inorg. Chem.* **2005**, *44*, 4237–4253.
- (13) Picquet, M.; Tkatchenko, I.; Tommasi, I.; Wasserscheid, P.; Zimmermann, J. *Adv. Synth. Catal.* **2003**, *345*, 959–962.
- (14) Barrosse-Antle, L. E.; Bond, A. M.; Compton, R. G.; O'Mahony, A. M.; Rogers, E. I.; Silvester, D. S. *Chem.—Asian J.* **2010**, *5*, 202–230.
- (15) Lee, S. Y.; Ogawa, A.; Kanno, M.; Nakamoto, H.; Yasuda, T.; Watanabe, M. *J. Am. Chem. Soc.* **2010**, *132*, 9764–9773.
- (16) Nakamoto, H.; Watanabe, M. *Chem. Commun.* **2007**, 2539–2541.
- (17) Susan, M. A. B. H.; Noda, A.; Mitsushima, S.; Watanabe, M. *Chem. Commun.* **2003**, 938–939.
- (18) Noda, A.; Susan, A. B.; Kudo, K.; Mitsushima, S.; Hayamizu, K.; Watanabe, M. *J. Phys. Chem. B* **2003**, *107*, 4024–4033.
- (19) Snook, G. A.; Greaves, T. L.; Best, A. S. *J. Mater. Chem.* **2011**, *21*, 7622–7629.
- (20) Thomson, J.; Gervasio, D. *214th Meeting of the ECS*, Honolulu, Hawaii; 2008, 67.
- (21) Zhao, C.; Burrell, G.; Torriero, A. A. J.; Separovic, F.; Dunlop, N. F.; MacFarlane, D. R.; Bond, A. M. *J. Phys. Chem. B* **2008**, *112*, 6923–6936.
- (22) Burrell, G. L.; Burgar, I. M.; Separovic, F.; Dunlop, N. F. *Phys. Chem. Chem. Phys.* **2010**, *12*, 1571–1577.
- (23) Ikeuchi, H.; Kanakubo, M. *Electrochemistry (Tokyo, Jpn.)* **2001**, *69*, 34–36.
- (24) Fletcher, S.; Horne, M. D. *Electrochim. Commun.* **1999**, *1*, 502–512.
- (25) Fletcher, S.; Horne, M. D. *RAM Electrodes - An Introduction*. DMR-1088, 3rd ed.; CSIRO Process Science and Engineering: Bayview Avenue, Clayton, Victoria 3168, Australia, August 1996; ISBN 0 642 20197 8.
- (26) Bernardini, G.; Zhao, C.; Wedd, A. G.; Bond, A. M. *Inorg. Chem.* **2011**, *50*, 5899–5909.
- (27) Wang, H.; Zhao, C.; Bhatt, A. I.; MacFarlane, D. R.; Lu, J. X.; Bond, A. M. *ChemPhysChem* **2009**, *10*, 455–461.
- (28) Saheb, A.; Janata, J.; Josowicz, M. *Electroanalysis* **2006**, *18*, 405–409.
- (29) Gritzner, G.; Kuta, J. *Pure Appl. Chem.* **1984**, *56*, 461–466.
- (30) Lagrost, C.; Carrie, D.; Vaultier, M.; Hapiot, P. *J. Phys. Chem. A* **2003**, *107*, 745–752.
- (31) Stojanovic, R. S.; Bond, A. M. *Anal. Chem.* **1993**, *65*, 56–64.
- (32) Hultgren, V. M.; Mariotti, A. W. A.; Bond, A. M.; Wedd, A. G. *Anal. Chem.* **2002**, *74*, 3151–3156.
- (33) Sukardi, S. K.; Zhang, J.; Burgar, I.; Horne, M. D.; Hollenkamp, A. F.; MacFarlane, D. R.; Bond, A. M. *Electrochim. Commun.* **2008**, *10*, 250–254.
- (34) Shiddiky, M. J. A.; Torriero, A. A. J.; Zhao, C.; Burgar, I.; Kennedy, G.; Bond, A. M. *J. Am. Chem. Soc.* **2009**, *131*, 7976–7989.
- (35) Barnes, E. O.; O'Mahony, A. M.; Belding, S. R.; Compton, R. G. *J. Chem. Eng. Data* **2010**, *55*, 2219–2224.
- (36) Bard, A. J.; Faulkner, L. R. *Electrochemical Methods: Fundamentals and Applications*, 2nd ed.; Wiley: New York, 2001.
- (37) Silverster, D. S.; Compton, R. G. *Z. Phys. Chem.* **2006**, *220*, 1247–1274.
- (38) Belieres, J. P.; Gervasio, D.; Angell, C. A. *Chem. Commun.* **2006**, 4799–4801.
- (39) Belieres, J. P.; Angell, C. A. *J. Phys. Chem. B* **2007**, *111*, 4926–4937.
- (40) Yoshizawa, M.; Xu, W.; Angell, C. A. *J. Am. Chem. Soc.* **2003**, *125*, 15411–15419.
- (41) Lee, J.; Yoon, S.; Hyeon, T.; Oh, S. M.; Kim, K. B. *Chem. Commun.* **1999**, 2177–2178.
- (42) McEwen, A. B.; Ngo, H. L.; LeCompte, K.; Goldman, J. L. *J. Electrochem. Soc.* **1999**, *146*, 1687–1695.
- (43) Xu, B.; Wu, F.; Chen, R. J.; Cao, G. P.; Chen, S.; Wang, G. Q.; Yang, Y. S. *J. Power Sources* **2006**, *158*, 773–778.
- (44) Nanjundiah, C.; McDevitt, S. F.; Koch, V. R. *J. Electrochem. Soc.* **1997**, *144*, 3392–3397.
- (45) Wachter, P.; Schreiner, C.; Zistler, M.; Gerhard, D.; Wasserscheid, P.; Gores, H. *J. Microchim. Acta* **2008**, *160*, 125–133.

- (46) Solangi, A.; Bond, A. M.; Burgar, I.; Hollenkamp, A. F.; Horne, M. D.; Ruther, T.; Zhao, C. *J. Phys. Chem. B* **2011**, *115*, 6843–6852.
(47) Kudo, A.; Miseki, Y. *Chem. Soc. Rev.* **2009**, *38*, 253–278.